water

MDPI

Article

Role of Grain Size Distribution and Pier Aspect Ratio in Scouring and Sorting around Bridge Piers

Takeyoshi Chibana *, Rose Quiocho and Kenji Watanabe

Faculty of Engineering, The University of Tokyo, Hongo7-3-1, Bunkyo-ku, Tokyo 1138656, Japan; requiocho@alumni.u-tokyo.ac.jp (R.Q.); watanabe@civil.t.u-tokyo.ac.jp (K.W.)
* Correspondence: chibana@hydra.t.u-tokyo.ac.jp

Abstract: Several bridge piers were visited, and their scour hole was characterized into three zones: scour, transition, and mound zones. The observed onsite sorting and scouring patterns were recreated through flume experiments with varying pier aspect ratio (1:1, 1:2, 1:4 and 1:6) and sediment geometric standard deviation (σ_g). The experiments showed that maximum scour depth decreased with non-uniformity; 52.7 mm, 20.2 mm, and 16.6 mm are the respective maximum scour depth of beds with σ_g = 1.4, 2.5, and 5.2. While aspect ratio has minimal effect on maximum scour depth values, it has noticeable effects on scour shape and asymmetry. The location of the lowest point of the scour shifted further downstream as σ_g increased. The number of occurrences where the location of the lowest point is outside the upstream cylindrical hemisphere is zero (0) for σ_g = 1.4, three (3) for σ_g = 2.5, and five (5) for σ_g = 5.2. The observed processes of upstream-to-downstream propagation of scour may explain the gradual decrease in fines on the surface, as well as the asymmetry of the scour, confirming the role of combined effects of grading of the bed material and piers' aspect ratio in the scour-forming process.

Keywords: bridge pier; local scouring; sediment grading; sediment sorting; pier aspect ratio

Citation: Chibana, T.; Quiocho, R.; Watanabe, K. Role of Grain Size Distribution and Pier Aspect Ratio in Scouring and Sorting around Bridge Piers. *Water* **2022**, *14*, 2066. https://doi.org/10.3390/w14132066

Academic Editor: Chang Lin

Received: 9 May 2022
Accepted: 23 June 2022
Published: 28 June 2022

1. Introduction

Countries located on the Pacific Ring of Fire are known to have a great number of rivers [1] and high sediment production rates [2]. These characteristics increase the possibility of occurrence of sediment disasters, hence putting importance upon understanding processes and interaction between the riverbed and artificial structures. As structures, piers are necessary to build infrastructures essential to accommodate human activities. Local scouring around the bridge pier is recognized as the one of the leading causes of bridge failure [3,4], and an array of studies, experimentally and numerically, have defined relationships of these parameters with maximum scour depths: flow velocity, flow depth, ratio of pier width and sediment size, pier aspect ratio, pier nose shape, pier cross-sectional shape, pier alignment, and foundation shape, among others [5–8].

It is noticeable that the majority of the research, conducted both in the past and in recent years, are focused on uniform materials, despite the undeniable effect of sediment non-uniformity and grading on scouring [8]. The bed materials of natural gravel rivers are known to be graded to fit log-normal, Talbot, or Bimodal distribution [9]. In terms of pier scouring, Nicollet and Ramette investigated a mixture of equal parts of three sizes of sands and found that a non-uniform bed will result in about 25% less scour than the scour of the individual components [10]. Ettema incorporated effects of grading by relating scour depth with the ratio of geometric standard deviation (σ_g) and median size (d50) [11]. It was found that scour depth decreases dramatically with σ_g/d50 if the ratio is above 0.3 under clear-water scouring. Chabert and Engeldinger defined the regimes of scouring: clear-water and live-bed [5]. Clear-water scours are scours formed due to local flow disturbance brought about by obstructions, such as piers. On the other hand, during live-bed

scour formation, bed materials are actively transported with or without obstructions. These types are separated by the ratio of the average approach velocity (U) and the critical velocity (U_c) to initiate motion of the median diameter (d50). The study concluded that for scours formed in clear-water regimes, depth increases with U/Uc, from a minimum of 0.5 and peaking at the ratio equal to 1 for beds made out of uniform sediments. Scours formed with U/U_c above 1 are considered live-bed scours. Baker extended the investigation of the effects of bed material grading under live-bed scouring [12]. Unlike earlier studies, recent publications are starting to investigate effects on scouring shape, rather than maximum scouring depth alone [13–16]. This shift has provided a more visual understanding for scour protection design and implementation. However, the relationship of sediment grading to scour geometry is yet to be explored; hence, being one of the relatively unexplored parameters, the effect of bed material grading on scouring has to be investigated.

Another phenomenon directly related to sediment non-uniformity is sediment sorting. Sorting is a phenomenon that is known to produce several riverbed structures that affect riverbed stability. Sediments are known to sort primarily by size and secondarily by shape [17]. Sorting and scouring are known to co-exist around artificial structures such as revetments and spur dykes on graded riverbeds [18–20]. Non-uniform bed topology and changes in flow patterns are known to influence sorting of bed materials [21], and both are known to exist around pier scours. Sorting is an important process that may influence stability of river bedforms [22]. Another phenomenon related to sorting is the formation of armor layers. Armoring is known to have a relationship with reduced mobility of bed materials [23,24]. A recent study by Pandey showed that armoring around circular piers reduced scour depth [25]. These previous studies, along with the notable observations on visited sites, only put emphasis on the importance of understanding the interaction of scouring and sorting with one another.

The effects of pier geometry as an equally important factor affecting the flow velocity and pressure have been investigated by various researchers including Hjorth, who focused on piers with equal length and width (circular and rectangular piers) through experiments [26]. A more recent experimental study by Vijayasree, observed scour geometry and flow vectors around piers with width-to-length ratio of 1:5, with varying cross-sectional shapes [16]. There is a wide range of experiments that related critical scour depths with the pier's properties such as cross-sectional shape, width, upstream curvature, alignment, and aspect ratio, among others. Using three different pier nose shapes (square, elliptic, and lenticular) and three different aspect ratios (1:1, 1:2, and 1:3), Lauren and Toch showed that the difference in scour depth is independent of pier aspect ratio but is heavily influenced by nose shape and angle of attack [27]. Effects of foundation shape, depth, and alignment of circular piers on scouring have been shown by Melville and Eghbali [14,28].

Based on the comprehensive literature review performed, there is an apparent research gap concerning the combination of the effects of grain size distribution and the pier's aspect ratio on scouring shape. Additionally, sorting and scouring are often observed simultaneously, and it is evident that these two processes interfere with one another. Hence, their interaction should be understood. Two core objectives have been chosen to bridge some of the apparent research gaps concerning scouring and sorting around bridge piers. The following are the research objectives for this study and their respective research questions:

- To understand and clarify the effects of bed material grading and pier geometry on scouring and sorting;
- To understand and clarify the interaction between local scouring and the process of sediment sorting.

2. Materials and Methods

In order to understand the role of grain size distribution in the sorting and scour-forming mechanism around bridge piers, field observations were coupled with flume

experiments to understand the mechanism. Field data collected during site observation are also necessary for scaling. The experiment was performed focusing on the interaction of sediments as a mixture with the pier. Sediment grading and pier geometry were set in a total of 12 combinations. Sorting behaviors of sediment during the scour-forming process were also observed.

2.1. Field Measurement and Observation

A total of nine (9) cylindrical piers of various aspect ratios were observed along 6 different gravel bed rivers in various regions in Japan. These six (6) rivers are the Tama River in Tokyo, the Nakatsu River and the Sagami River in Kanagawa, the Ara River in Niigata, and the Otofuke River and the Satsunai River in Hokkaido. The dimensions of the piers were measured, while the sorting patterns and scour shapes were observed.

In each river, line sampling was performed on gravel bars proximate to observed piers, to determine grain size distribution of the riverbed material. The line sampling was performed by using graduated measuring tape to lay out two 50 m lines, one near the water line and another on top of gravel bar. The intermediate diameters of sediments that fall under 1 m mark intervals from 0 m–50 m were measured [29], totaling to 102 readings per site. During events where the meter mark falls over debris or vegetation, measurement was noted as an error. These collected data were used for experiment design and scaling. The characteristics of the grain size distribution of the visited river reaches are summarized in Figure 1 and Table 1. The visited rivers are a mixture of three major basin geologies in Japan: accretionary complex, volcanic rock, and granite rock. Despite the wide range in d50 among visited rivers (23.0–74.6 mm), the geometric standard deviation (σg) among rivers is consistent (2.11–2.36) except two outliers. Geometric standard deviation (σg) equates to the square root of the ratio of d16 and d84. It is noteworthy that the outliers, both the narrowest and widest distribution, fall under volcanic rock basin geology. The maximum sediment size of the Otofuke River is larger than that of the Nakatsu River. However, the mean sediment diameter of the Nakatsu River is larger due to the large amount of fines in the Otofuke River. These characteristics of diverse grain size distribution between two rivers represent the diversity in sediment size distribution in rivers running through volcanic rock.

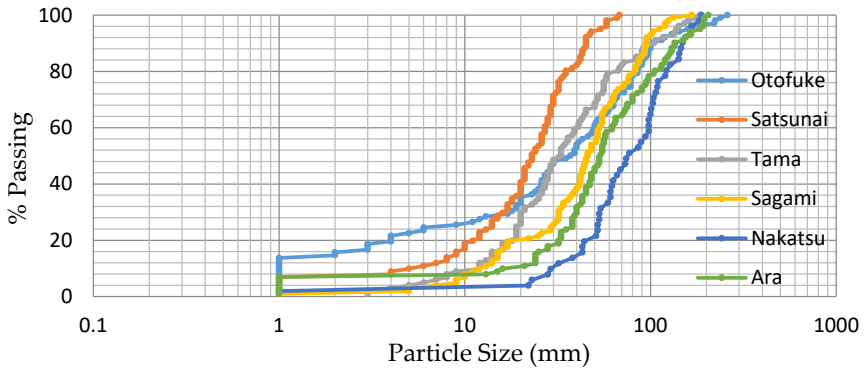

Figure 1. Grain Size Distribution Curves of the Visited Rivers.

Table 1. Properties of the Grain Size Distribution.

	Otofuke	Satsunai	Tama	Sagami	Nakatsu	Ara
d50(mm)	37.0	23.0	32.5	46.0	74.6	53.5
σ_g (mm)	6.24	2.11	2.26	2.36	1.73	2.19
Basin Geology	Volcanic Rock	Accretionary Complex	Accretionary Complex	Accretionary Complex	Volcanic Rock	Granite Rock

2.2. Flume Experiments

The sizes of the piers and bed material of this experiment are scaled based on site conditions. The ratio of the median sediment size of the bed material (d50) and the width of the pier (b) was based on actual field conditions. For this experiment, the value for the measurement in the Satsunai River (b/d50 = 35 (b = 0.8 m, d50 = 0.023 m)) was used, as it falls within the prescribed range of b/d50 values of 25 to 50 [28]. The maximum width of the pier was limited to 10% of the width of the flume to avoid flow contraction, consistent with past studies [30]. A total of three sets of bed materials were prepared. All three have the same median size (d50) of 0.7 mm but with varying geometric standard deviation (σ_g). The plot of the grain size distribution (GSD) curves in log scale is as shown in Figure 2**.** The bed materials used for this experiment have geometric standard deviation equal to 1.4, 2.5, and 5.2, representing different conditions. The value of 2.5 corresponds to visited gravel rivers (σ_g = 2.11–2.36) apart from two outliers: the Nakatsu River (σ_g = 1.73) and the Otofuke River (σ_g = 6.24). GSD 1 (σ_g = 1.4) represent uniform sediments, while GSD2 (σ_g = 2.5) and GSD3 (σ_g = 5.2) are mixed sediments of increasing grading wideness. Both GSD2 and GSD3 are colored sand mixtures, composed of unique colors for each size fraction. This is to visually identify size sorting around piers.

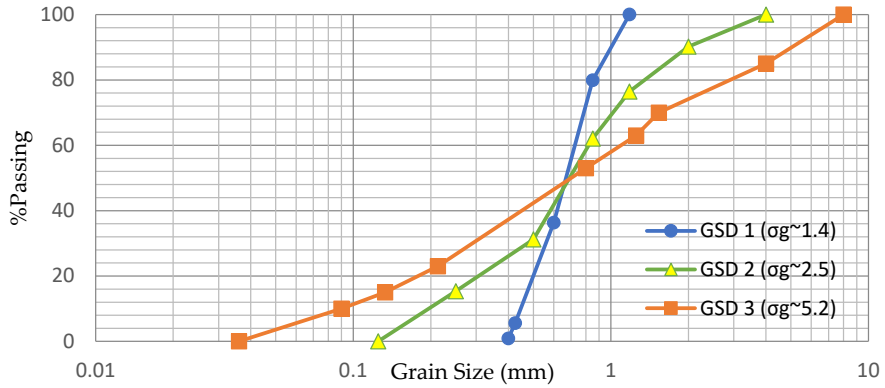

Figure 2. Grain Size Distribution Curves of Bed Materials for Experiment.

Additionally, four blunt-nosed cylindrical piers with varying width-to-length ratio (aspect ratio) were also prepared. The width of all piers is 2.5 cm. Four different aspect ratios (1:1, 1:2, 1:4, 1:6) were used to illustrate their effect, because a range of values were frequently observed onsite. The piers were made out of PVC and concrete composites and were painted and graduated in 5 mm accuracy along midpoints of all 4 sides, as shown in Figure S1.

In this experiment, a 5 m long by 0.3 m wide tilting flume was used. The flume was tilted on a constant slope of 1/1000. This slope was chosen to alter depth of flow, as depth of scour is related to the ratio of flow depth and pier width in most literature. The live-bed is 3.5 m long, 0.3 m wide, and 0.1 m deep. The schematic and actual setup of the flume are in Figure S2. A total of 48 runs with combination of 2 sets of discharge (Q1 and Q2), 3 sets of grain size distribution (GSD1, GSD2, and GSD3), 4 sets of aspect ratio (1:1, 1:2, 1:4, and 1:6), and 2 durations of flooding (T = 2 h and T = 4 h) were performed. Half of the runs started with a leveled bed, while the rest were continuations of previous runs. Upon completion of initial flume setup, the pump was then turned on at either Q1 (3.6 L/s) or Q2 (1.8 L/s) continuously for 1 h, then turned off briefly for 10 min, and then turned on again for another 1 h. Q1 is the maximum capacity of the flume pump, while Q2 was chosen to create a flow depth sufficient to accommodate camera views during runs. Cycles of flooding were performed to observe brief periods of unsteady flow.

Before measuring the topography of the bed, the flume was left overnight to ensure that the bed was completely dried out and free of pools of water that may interfere with the laser readings. The elevation of the bed was measured using a laser range finder with 1.5 mm accuracy, on 1 cm by 1 cm grid. The pump was then turned on at the same discharge for another 2 h, in two 1 h intervals, similar to the previous run. In a similar manner, the elevation of the dried bed was re-measured. The bed was releveled prior to repeating the cycles of discharges and measurements. This was done for all 12 combinations of bed materials and pier.

Two discharges, Q1 and Q2, were chosen with U/Uc (the average approach velocity over the estimated critical velocity to initiate motion of the median diameter) between 0.5 and 1 to facilitate clear-water scouring. The properties of the flow are described in Table 2. Using Froude similarity, the ratio of depth, pier width, d50, and time of the flooding phenomenon on the actual river (field) was conserved on the physical model (flume). Velocities of flow in the flume were calculated using the discharge and depth data collected during experimental runs. Velocities in the field were estimated using Manning's equation, imputing the depth estimated by the depth measured in the flume, the river width measured from satellite images retrieved from Google Earth©, and literature value of roughness 0.030 of a typical gravel bed river [31]. Lastly, the average velocities (U) of Q1 and Q2 chosen for the experiment were calculated to be 0.25 m/s and 0.19 m/s respectively. Then, the value of roughness in the flume was estimated as 0.014. The velocities correspond to U/Uc of 0.67 and 0.55, which both fall within the range of 0.5–1.0 to satisfy clear-water scouring conditions. Uc is estimated by Melville's method. Ref. [32] Corresponding discharges for Q1 and Q2 in the actual river are estimated as 803 m^3/s and 368 m^3/s, respectively. The actual data of river discharge were collected from the online database of the Ministry of Land Transport and Tourism (MLIT) to see the equivalence of the experiment and field. At the water gauge station adjacent to the study site, maximum and mean annual maximum discharge from 1968 to 2020 are 1014 m^3/s and 487 m^3/s, respectively. These are slightly larger than the discharge estimated from the flume experiment, but actual riverbed slope is steeper than the flume. Hence, the actual sediment transport is considered to be more active than the condition in the flume.

Table 2. Flow Properties for Experiment and Corresponding Flow Regimes in the Satsunai River.

	Width (m)	**Depth (m)**	**Pier Width (m)**	**d50 (mm)**	**n**	**Velocity (m/s)**	**Q (m^3/s)**	**Uc (m/s)**	**U/Uc (m/s)**
Exp Q1	0.3	0.05	0.025	0.7	0.014	0.25	0.0038	0.37	0.67
Satsunai River (Q1)	350	1.6	0.8	23	0.03	1.4	803	2.14	0.67
Exp Q2	0.3	0.03	0.025	0.7	0.014	0.19	0.0017	0.34	0.55
Satsunai River (Q2)	350	1	0.8	23	0.03	1.1	368	1.97	0.53

3. Results

3.1. Field Measurement and Observation

Areas proximate to piers were observed, with a focus on sediment sorting and scour shape. It is known in the literature that flow around bridge piers is distinguished by the horseshoe and the wake vortices on the upstream and downstream sides, respectively. Despite the differences in the grain size distribution among visited sites, a distinct pattern was observed. The characteristic features of the scours around the piers may be divided into three different zones, as shown in Figure 3.

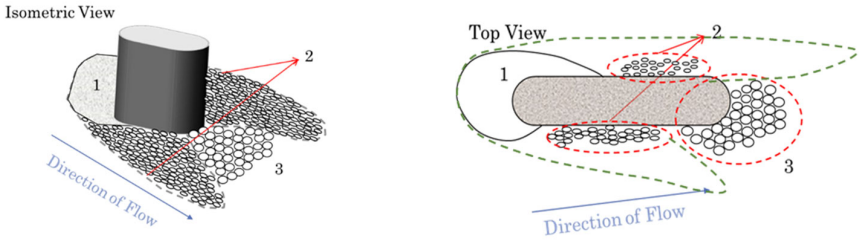

(**a**) (**b**)

Figure 3. Illustration of Typical Scour and Sorting Pattern showing Zones 1, 2, and 3: (**a**) Isometric View; (**b**) Top View.

Zone 1, shown in Figure 4a, is the region just upstream of the pier. This zone is characterized by steep downward sandy slopes with gravel deposits on the lowest part. Water line marks are also noticeable on several visited sites, signifying gradual reduction in water level on the scour hole. Zone 2, shown in Figure 4b, is the section along both pier sides. This region acts as the transition between zone 1 and zone 3. The characteristics of zone 2 include a relatively gentler positive slope and gradual increase in sediment size from upstream to downstream. More often than not, the elevations of the left and right sides of zone 2 are unequal. Another feature of zone 2 that is noteworthy is its compactness and the concentration of sediments with shape irregularity that seems to affect its stability. Zone 3, shown in Figure 4c, is the area downstream the pier characterized by a pile of rounded sediments, with noticeable absence of fines. Due to these features, this region is rather unstable. These observations support previous literature's findings that sorting is indeed primarily influenced by size but is also secondarily influenced by shape [17].

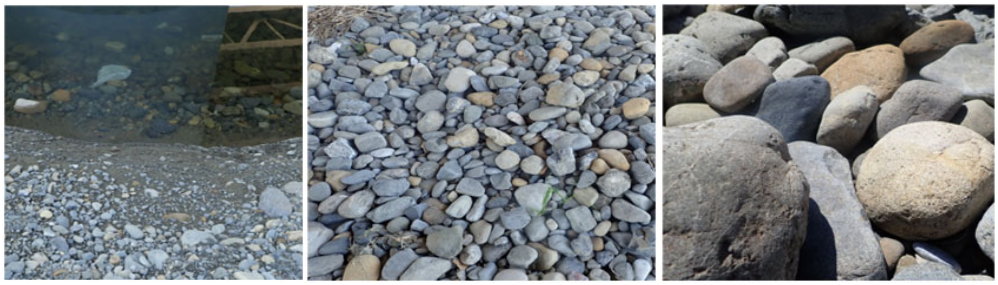

(**a**) (**b**) (**c**)

Figure 4. Sediments around a Pier: (**a**) Zone 1; (**b**) Zone 2; (**c**) Zone 3.

However, the condition and location of zone 3 vary among visited sites. It was noted that visited piers with 1:1 aspect ratio (circular) tend to have scours all around, with zone 3 located further downstream. Piers with a longer aspect ratio tend to have enough transition length and usually have zone 3 more proximate to the piers, with some having zone 3 located just downstream of the pier. However, it is difficult to conclude whether this observation is solely dependent on aspect ratio due to the difference in site conditions, specifically in flow properties. A set of piers with different aspect ratios were observed to behave in this manner, although they were only several hundred meters apart. We may assume that these piers are subjected to similar site conditions, proving the influence of the piers' aspect ratio on zone 3's condition.

Apart from the noticeable size and shape sorting of sediments around the pier, the asymmetry of the scour hole shown in Figure 5 was also noteworthy. Pier alignment relative to the direction of flow was initially suspected as the main, if not the sole, factor in the asymmetry. However, it was noted that the location of the higher or lower side is not consistent among visited sites, even though all piers are located on the left flood plain.

Despite this observation, we cannot ignore the influence of flow alignment on scour asymmetry, as was already proven by previous studies [14].

(**a**) (**b**)

Figure 5. Asymmetry of Scouring and Deposition around a Pier along the Ara River. (**a**) Looking Upstream (**b**) Looking Downstream.

3.2. Flume Experiment

The results of the flume experiments may be divided into two parts: Scouring and Sorting. Apart from the comparison of maximum scour depth in relation to bed grading and a pier's aspect ratio, this study is also interested in the geometry of scouring, with a focus on asymmetry. Another focus related to scouring is on the effect of transition length on downstream conditions of the pier.

3.2.1. The Effects of Bed Material Grading and Pier Geometry to Scouring

Maximum-scour-depth prediction has been a key component in designing river bridges. The summary of the maximum scour depths and deposition relative to the initial bed elevation in all runs is in Table 3. Scour depth for lower discharge (Q2) ranges from 21.25–32.85 mm for GSD1, 6.7–10.3 mm for GSD2, and 3.94–9.3 mm for GSD3. On the other hand, for the higher discharge (Q1), the ranges are 43.65–51.5 mm, 14.85–20.2 mm, and 9.2–16.6 mm for GSD1, GSD2, and GSD3, correspondingly. The increase in scour depth with increased discharge was expected and consistent with literature. The U/U_c ratios of Q1 and Q2 of this study are 0.67 and 0.55, respectively. Since both are below 1, both cases are under clear-water scouring and are anticipated to be below the critical equilibrium scour depth. Note that Chabert and Engeldinger's conclusions [5] were based on data of uniform sediment experiments; nonetheless, the same pattern was observed for graded materials. Clear-water scour depths are also expected to increase until equilibrium time at steady discharge [28]. However, since cycles of flooding were employed in this study, there were brief periods of unsteady flows in between extended steady flow. Even if steady flow conditions are rather longer than the unsteady intervals, the data showed fluctuating depth heights. For uniform sediments (GSD1), increasing scour depth was observed on high flows (Q1), yet the trend was reversed for low discharge (Q2). Scour depth of mixed-sediment beds (GSD2 and GSD3) is rather random with respect to time. However, we can see that both mixes behave similarly, either increasing or decreasing, for high discharge.

Table 3. Flow Properties for Experiment.

Pier (Aspect Ratio)	Time (h)	Discharge	Max Scour Depth (mm)			Max Deposition Height (mm)		
			GSD1	GSD2	GSD3	GSD1	GSD2	GSD3
1 (1:1)	2	2(1.8 L/s)	31.8	9.4	9.3	15.85	4.45	6.5
1 (1:1)	4	2(1.8 L/s)	24.4	8.95	6.55	14.35	4.2	7.3
1 (1:1)	2	1(3.6 L/s)	48.15	18.4	16.6	7.05	3	5.15
1 (1:1)	4	1(3.6 L/s)	51.5	20.2	13.35	4.85	4.25	4.75

2 (1:2)	2	2(1.8 L/s)	32.85	7.9	3.94	14.5	6.45	2.05
2 (1:2)	4	2(1.8 L/s)	21.25	10.3	4.5	7.2	4.25	2.6
2 (1:2)	2	1(3.6 L/s)	48.2	19.85	9.9	6.05	4.75	3.9
2 (1:2)	4	1(3.6 L/s)	52.7	16.4	9.2	3.85	6.05	4.5
3 (1:4)	2	2(1.8 L/s)	28.85	8.99	5.35	11.6	7.71	3.8
3 (1:4)	4	2(1.8 L/s)	22.4	8.6	4.9	11.6	6.5	3.55
3 (1:4)	2	1(3.6 L/s)	43.65	16.7	10.55	7.25	8.45	6.0
3 (1:4)	4	1(3.6 L/s)	51	17.94	9.7	3.0	8.76	6.1
4 (1:6)	2	2(1.8 L/s)	32.25	6.7	4.8	8.8	5.25	4.35
4 (1:6)	4	2(1.8 L/s)	23.45	7.25	5.35	9.45	5.3	4.4
4 (1:6)	2	1(3.6 L/s)	45.9	14.85	10.8	1.95	7	4.75
4 (1:6)	4	1(3.6 L/s)	48.95	15.7	9.25	1.95	5.65	4.75

The data also clearly show that the maximum scour depths are much lower on mixed-sediment beds in reference to the standard, at the same flooding conditions. This observation is consistent with various experimental studies that related non-uniformity to reduced bed transportation rate [33] and scouring depth [10]. These studies, however, used sediment mixes with rather straight distribution curves by mixing 2–3 component sizes. Unlike these studies, Ettema quantified the non-uniformity and grading of bed materials by using the geometric standard deviation (σ_g) as an index [11]. The study related scour depth with the ratio of geometric standard deviation (σ_g) and median size (d50). It was found that scour depth decreases dramatically with σ_g/d50 if the ratio is above 0.3. The σ_g/d50 of the bed materials of this study are as follows: GSD1 = 1.62, GSD2 = 3.38, and GSD3 =7.03. Since σ_g/d50 of all bed materials satisfy the condition, and knowing that d50 is a constant for all sediment mixes, we expect a decreasing trend based on plotting scour depth versus σ_g. Figure 6 shows that scour depth decreases dramatically as σ_g increases, for both high and low discharge.

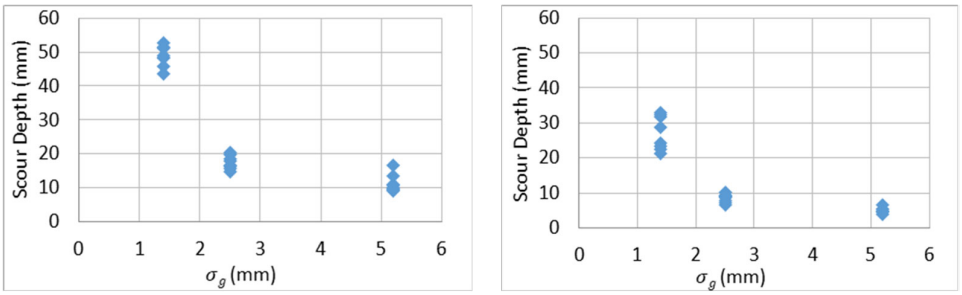

Figure 6. Plot of Scour Depths for Different Bed Material Gradation: (**a**) Q1; (**b**) Q2.

Apart from maximum scour depth, scour geometry is another interest of this study. Scour geometry is an important consideration for placing scour protection measures. However, the majority of the studies focusing on scour geometry are only investigating its relationship to flow alignment. Figure 7 shows the profiles of channel beds just upstream the piers, for all aspect ratios. The line in blue hues shows the profiles for GSD1, green-hued lines are for GSD2, and yellow-hued lines are GSD3 outlines. The figure clearly illustrates the apparent decrease in scouring in terms of both depth and width, with increased non-uniformity or wideness of distribution curve. Laursen and Toch found that for blunt-nosed piers aligned with the flow, aspect ratio (1:1, 2:3, 1:2, and 1:3) has minimal effects on scour depth on uniform beds [27]. The profiles of P1–P4 (1:1, 1:2,1:4, and 1:6) on GSD1 show minimal difference in scouring, both in terms of shape and depth. This observation confirms and extends Lauren and Toch's findings to piers with longer aspect ratios. However, unlike uniform sediments, the combined effects of aspect ratio

and grading on scour depth have not been analyzed well. The results suggest that aspect ratio has very limited influence on scour depth in the same bed material. However, grading and aspect ratio have notable implications for scour geometry. We can see that profiles for GSD2 and GSD3 are more varied relative to GSD1. The effects of grading on scour shape were manifested in the irregularity of the profiles along line 1, especially for longer piers. The resulting profile of channel beds just upstream the piers, for all aspect ratios, for lower-discharge Q2 is available in the Supplemental Material Figure S3.

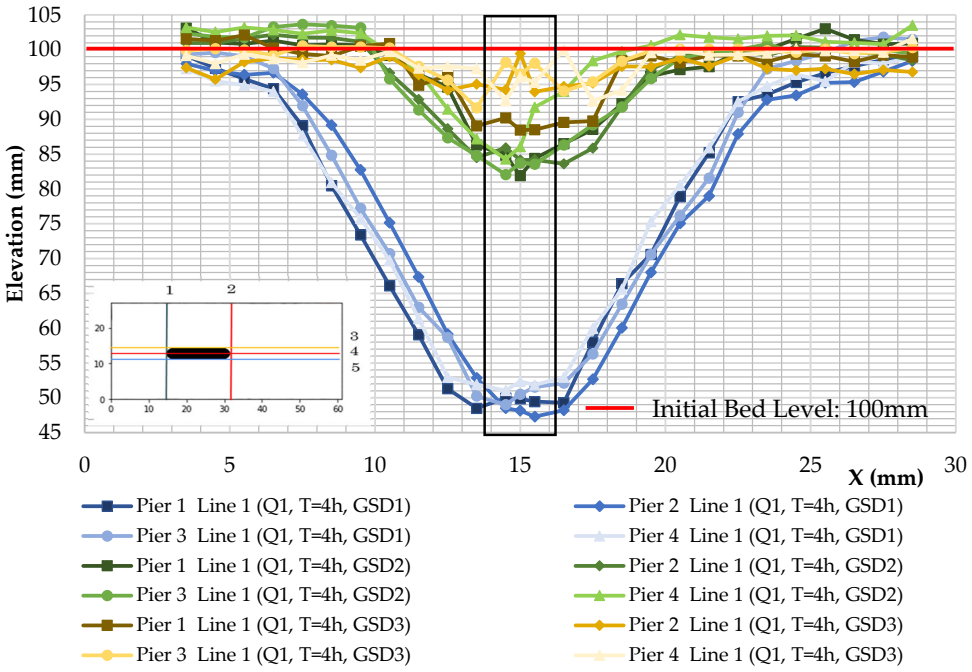

Figure 7. Cross-Section Profile along Line 1 for all Aspect Ratios and GSD (Q1, T = 4 h).

Apart from the profiles along line 1, the topology of the bed proximate the pier may clearly illustrate the effect of aspect ratio and grading on scouring asymmetry. Figures 8–10 show the shape of the developed scours around piers in different bed materials, after the same flooding conditions. We can see how the extent of scouring, in terms of area, was greatly reduced as the σ_g of the bed material increased. The irregularity of elevation contours is also observed to be increasing with σ_g.

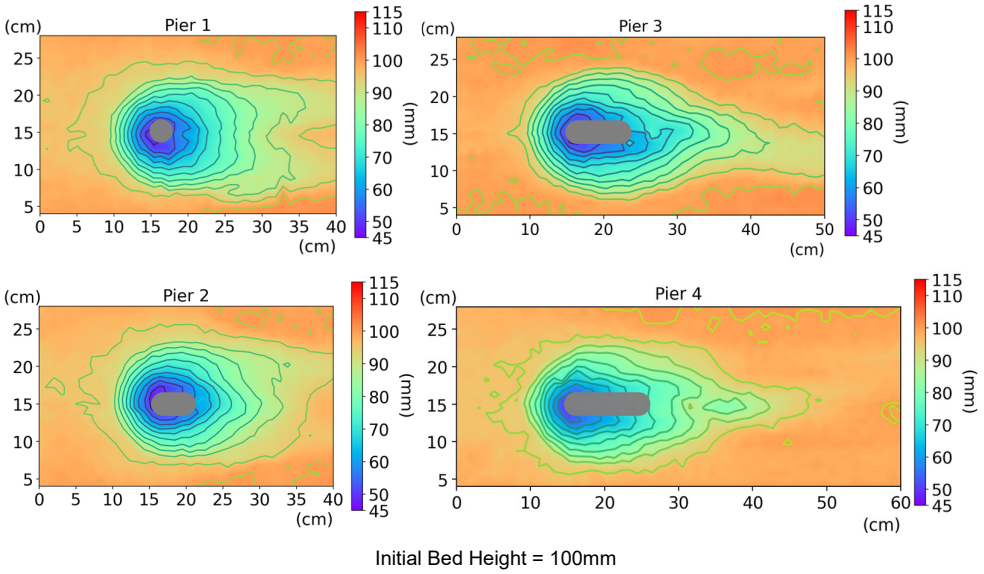

Figure 8. Bed Topology around Piers on GSD1 (Q1, T = 4 h).

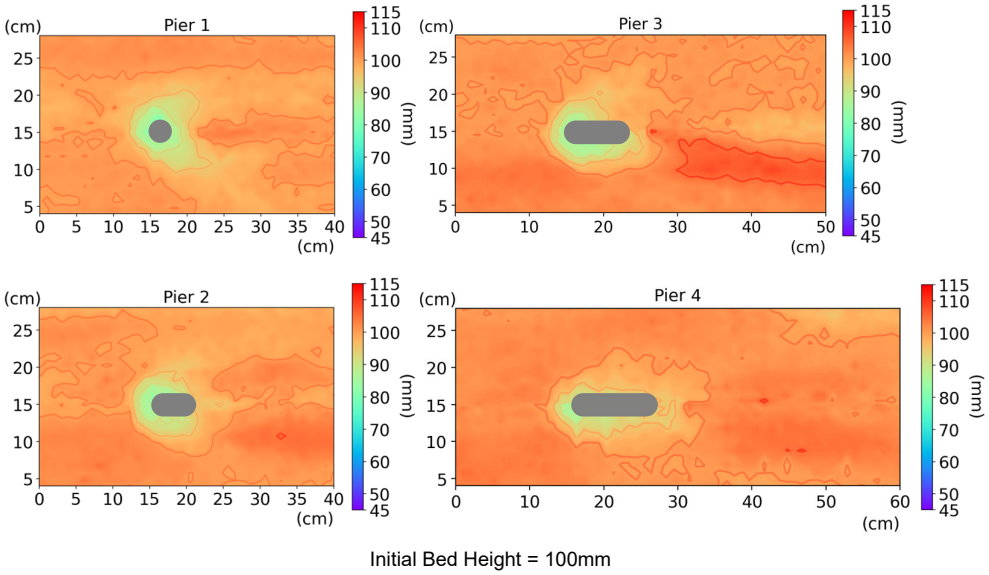

Figure 9. Bed Topology around Piers on GSD 2 (Q1, T = 4 h).

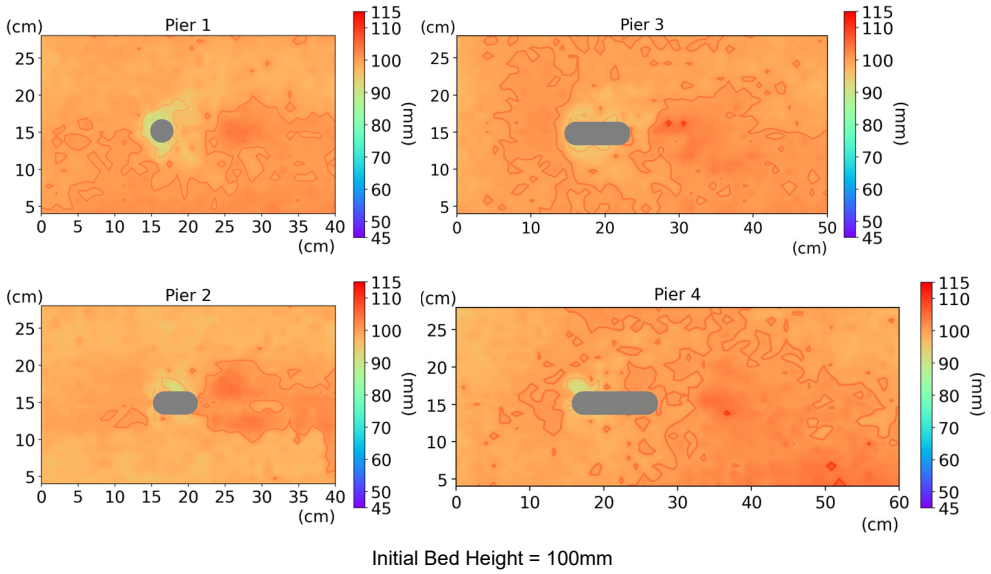

Figure 10. Bed Topology around Piers on GSD 3 (Q1, T = 4 h).

Figure 8 shows that aspect ratio has minimal impact on scour geometry upstream of the pier for uniform bed materials (GSD1). The extent of scour in terms of width is also unaffected, and the location of the lowest contour remains around the upstream side. However, the extent of scouring in terms of length increases with aspect ratio. Width and depth of scour along the profile just downstream of scour are visibly affected by the transition length. The planar shape of the scour boundary shifts from horseshoe to tilted teardrop.

Figure 9 shows the topology of the scours developed around piers on GSD2. In contrast to Figure 8, Figure 9 clearly shows that scour holes in graded bed tend to be asymmetric as length of pier increases. Unlike uniform materials, the extent of scour width just upstream the pier varies with aspect ratio in the case of GSD2. Clear asymmetry of the scour hole was observed in P3 and P4 in particular. In the case of P3, the width of the scour on the left (Y = 15–30 cm) is relatively wider than on the right side (Y = 0–15 cm). In terms of length, the scour on the right side compensates for its width deficit, as it appears to have greater coverage, almost reaching the downstream end of P3. On the other hand, the left side's scour terminates around the midpoint of the pier length. For P4, both the width and length of the scour on the left side are greater than on the right side.

Figure 10 illustrates the bed conditions proximate to piers on GSD3. Unlike GSD1 and GSD2, the scour upstream of the pier in GSD3 is rather unclear on all piers, apart from P1. The location of the lowest contour is also rather uncertain. Note that the largest size fraction of this bed material has a median size of 8 mm, which is roughly 1/3 of the pier's width. This size may have also meant it acted as obstruction and induced scour around it as well. For GSD1 and GSD2, a pier's aspect ratio appears to influence the unevenness of the scour as piers become longer. However, no pattern was observed for GSD3 due to its innate stability, producing a rather irregular and minimal local scouring.

The resulting contours for GSD 1, 2, and 3 on lower discharge Q2 are shown in the Supplemental Material Figures S4–S6, respectively.

Identifying the location of the lowest point of the scour is as important as predicting the maximum scour depth. Typical scour protection measures were placed all around circular piers or around the upstream nose of the pier for longer aspect ratios. However, the results of this study suggest that even at zero angle of attack or with pier perfectly aligned with the flow, scour asymmetry may be formed on graded beds. Figure 11 shows the plot

of the locations of the lowest points for each run, relative to the piers. These locations were classified into two regions: within and outside the upstream cylindrical hemisphere. This division was chosen to classify whether or not the identified location of the lowest point of the scour is covered by typical placement of scour protection measures for piers perfectly aligned with flow. Out of all the 48 runs, there were 8 cases where the location of the scours' lowest point was located outside the hemisphere of the upstream pier nose (X > 16 cm). Another noteworthy result is the distribution of these 8 cases among three bed materials. The number of cases where the location of the lowest point of the scour was shifted to further downstream was found to increase with σ_g. Some points are overlapping, but out of 16 cases per bed material grading, GSD1 has zero cases (0%), GSD2 has three cases (18.75%), and GSD3 has the most at five cases (31.25%). Even though the prior results show that graded bed materials produce shallower scours, asymmetry became more prominent for graded beds consequently. This finding is particularly important, since the combined effects of grading and aspect ratio were yet to be investigated in view of scour asymmetry.

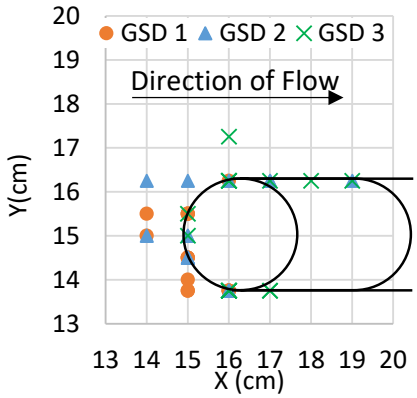

Figure 11. Plot of the Locations of Lowest Points of Scours. (Some plots are overlapping.)

Figure 12 shows the profile along the centerline that is Line4 in the figure, downstream of the piers. For high flow (Q1), we can see that shorter piers (P1 and P2) behave similarly, as is shown in Figure 12a. For both GSD1 and GSD2, the lowest point of the scour is directly downstream P1 and P2. The scour forms a positive upward slope, gradually recovering to initial bed height. On the other hand, for longer piers (P3 and P4), a negative downward slope was formed on both GSD1 and GSD2. For uniform beds (GSD1), the downstream side of the pier was scoured, but the location of the lowest point was pushed further downstream, before recovering to initial bed height. In contrast, deposition was observed downstream of P3 and P4 for GSD2.

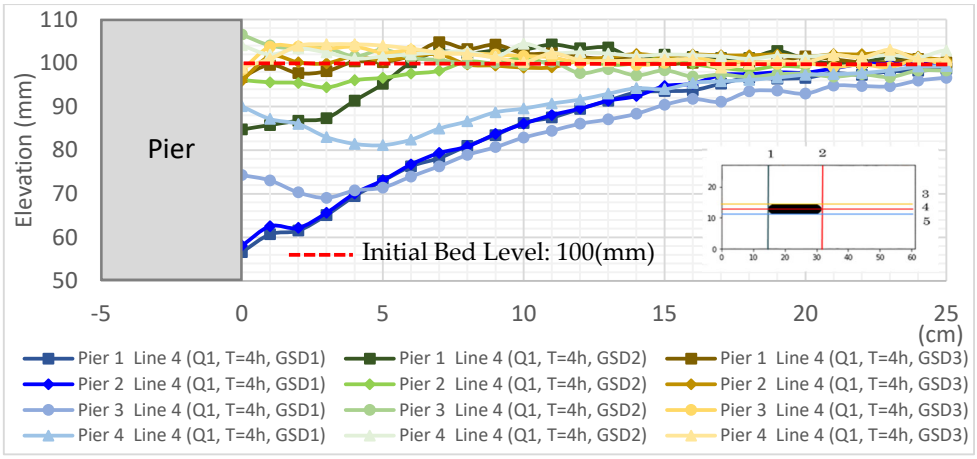

(**a**)

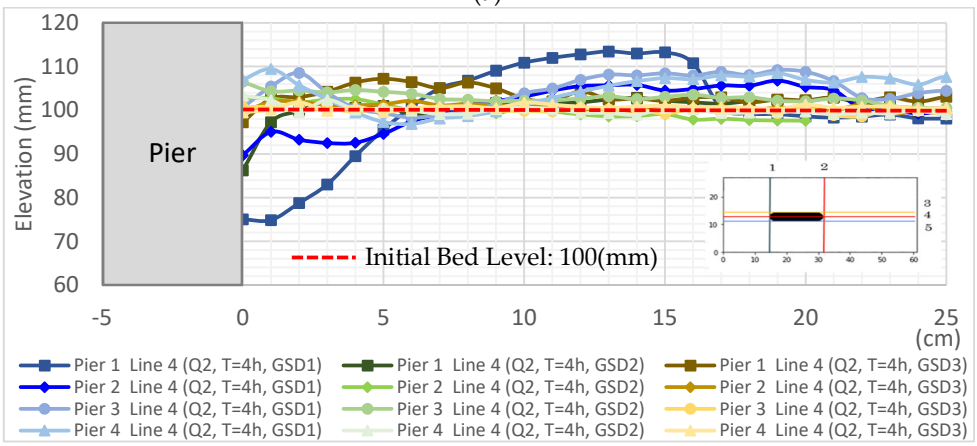

(**b**)

Figure 12. Elevation Profile along Line 4 (GSD1, GSD2, T = 4 h): (**a**) Q1 (Higher Discharge); (**b**) Q2 (Lower Discharge).

For the lower discharge (Q2), only the condition downstream of the circular pier (P1) was different from the rest, as is shown in Figure 12b. The profile just downstream P1 is characterized by a positive upward slope, but instead of recovering only until initial bed height, deposition was observed further downstream. The positive slope decreases dramatically after passing the initial bed height. For the rest of the piers, apart from P2 in GSD1, deposition was observed just downstream the pier. A short positive slope was created before inflecting twice, forming a shallow pool in between unequal amounts of deposits. For uniform sediments, a dune-like deposit was formed downstream before returning to initial bed height.

These observations suggest that the situation downstream the pier is a function of three different variables: approach velocity, pier length, and bed stability. Approach velocity and bed stability control the extent of scouring, hence determining whether scouring would reach the downstream side and fully encircle the pier. Pier length and approach velocity are the factors affecting reconnection velocity and the formation of wake vortices. Faster reconnection velocity will form greater turbulence and stronger wake vortices. Higher turbulence alters the situation downstream of the pier in two ways: first, it inhibits deposition of finer sediment fractions from supply upstream, and second, turbulent wake selectively suspends and entrains existing fines in place. A very small stagnation area was created in several cases when the flow reconnects further downstream. This area allows deposition or retention of finer sediment fractions. These observations will be further

discussed in the following section, as these are closely related to sediment size distribution around piers.

3.2.2. The Effects of Bed Material Grading and Pier Geometry on Sorting

Onsite, series of local fining and coarsening were observed surrounding the pier and its scour hole. Most of the patterns observed onsite were replicated in the experiment; however, some are not, primarily due to limitations on equipment capacity. For the replication in the flume, the bed material used for GSD2 and GSD3 were size color-coded to facilitate spatial size distribution through visual observation. GSD2 is composed of six (6) colors with diameter sizes ranging from 4–0.25 mm. The wider GSD3 has eight (8) component colors from 8 mm to 0.09 mm.

Figure 13 shows the planar view of the bed proximate to the pier in the case of Pier2 as the representative case, before and after four cycles of flooding. The case in GSD2 under Q1 shown in Figure 13a represents the widest extent in terms of change in the surface grain size distribution. Sediment fractions finer than the mixture's median size (d50 = 0.74 mm), blue (d50 = 0.5 mm) and maroon (d50 = 0.25 mm), were deposited along the majority of the channel width, apart from areas near flow turbulence (upstream and downstream of pier) and unequal velocity due to contact (pier sides and channel banks/walls).

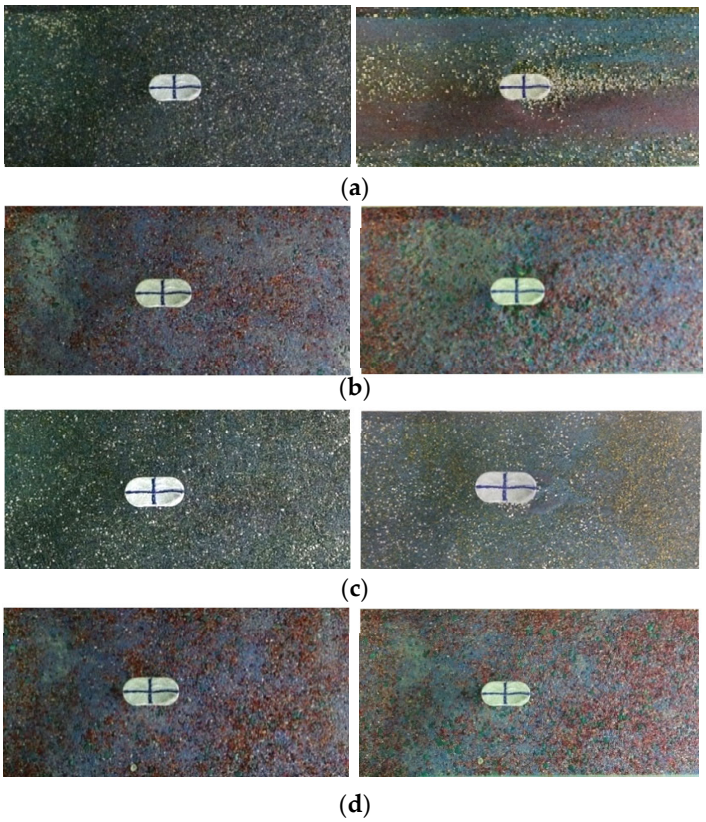

Figure 13. Top View of Bed Condition near the Piers. Left: Before; Right: After. (**a**) GSD2 and Q1; (**b**) GSD3 and Q1; (**c**) GSD2 and Q2; (**d**) GSD3 and Q2.

The case in GSD3 under Q1 shown in Figure 13b, however, is comparatively more stable as a mixture. Supply of sediments from upstream was limited to permit deposition. As such, existing finer fractions on the surface were selectively entrained, consequentially retaining and exposing larger grains, resulting in increased surface roughness of the bed. Visually, we can see a decrease in white (d50 = 0.09 mm) patches, while green (d50 = 8 mm) and bright red (d50 = 4 mm) are increased. This observation is not limited to areas

with turbulent flow but applies to the entire channel width. It is also noteworthy that the median size of the largest grain fraction (green) is 8 mm, which is roughly 1/3 of the size of the pier. Once exposed, these grains could individually act as submerged obstructions, creating their own local scour surrounding them.

Unlike the effects of higher discharge (Q1), the influence of Q2 on the surface grain size distribution is rather limited and local, in both GSD2 and GSD3 (see Figure 13c,d). It is observed that most of the materials transported from the scour formed just upstream of a pier are deposited either along the pier's side or downstream. The deposits form predominantly blue (d50 = 0.5 mm) and red (d50 = 0.25 mm) trails smeared along the flow direction. Another noticeable feature is the formation of several wave-like clusters of green (d50 = 2 mm) and yellow (d50 = 1.18 mm) sediments, which increased the overall unevenness of the bed. In particular, the case in GSD3 under Q2 shows the least change among the sets of before and after images. The stability of the bed material mixture (GSD3) and the weakness of the flow (Q2) both contributed to the seemingly unchanged surface condition of the bed. Scours are formed, but they are not very defined; hence, the supply of transported material from the developed scour holes was rather limited to create a visible trail similar to cases in GSD2. Several factors affect the conditions downstream of the pier, one of which is the stability of the bed. As observed, bed stability increases with σ_g. Based on the observations in Figure 13, we can say that the conditions downstream of the pier are related to the size of the scour developed upstream, as it serves as a primary sediment source.

Figure 14 shows the conditions upstream of the piers. Figure 14 clearly shows that the sorting or the distribution of sediments, upstream of a pier, particularly along the scour slope, is predominantly influenced by discharge intensity, while the pier's aspect ratio comes secondary with rather minimal contribution. For both the first and second rows, we can see clear coarsening along the direction of flow. The lowest portions of the scours are usually filled with the largest 1–2 fractions, with size decreasing along the scour slope as the elevation increases. Indistinct concentric rings of sediments are formed along the slope. It is noticeable that the mobility of the largest fraction to move towards downstream is influenced by the length of the pier. As Figure 14 shows, it is noticeable that the respective largest fractions of GSD2 and GSD3, white (GSD2, d50 = 4 mm) and green (GSD3, d50 = 8 mm), were significantly less behind (upstream) Pier1 compared to other piers under Q1. It was observed that it is easier for sediments to be transported in front of (downstream) Pier1, since the scour depth around the entire pier is almost equal. Transition length, which is equal to pier length, is also shortest; hence, reconnection velocity and turbulence downstream the pier are strongest. The sorting on lower discharge (Q2) for both bed materials is relatively less prominent compared to their Q1 counterparts. Fractions that are light enough are suspended by the vortex system and are redeposited or transported based on size. The primary supply of sediments is from the area just upstream the hemisphere of the pier nose. As the depth of this area increases, the area of scour increases as well. This is due to the subsequent sliding-slope failure due to lack of support to maintain the internal angle of friction or the static angle of repose (ϕ) of the bed material. As the scour progresses, the resuspension and redeposition continues until the maximum planar extent of the scour is achieved. For the case of Q1, the flow is sufficiently fast to create a vortex system turbulent enough to suspend even the largest fractions of GSD2, which is d50 = 4 mm. However, the discharge is not sufficient to suspend the largest fraction of GSD3, which is double the size (d50 = 8 mm). Note that when a certain size is not suspended, that size fraction, once fully detached off the bed matrix, would slide through the scour slope and be deposited towards the nearest lowest point by gravity. That is the reason as to why the radial distribution of the largest fraction was more evenly distributed in the GSD2 relative to GSD3.

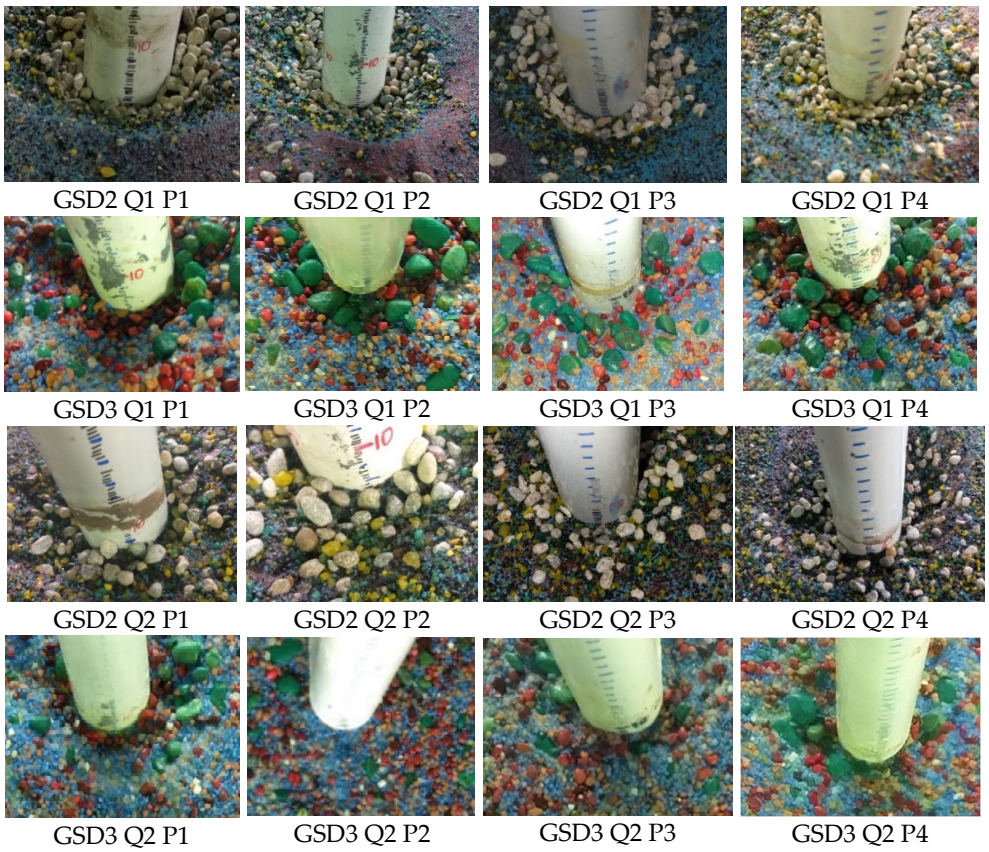

Figure 14. Situation just upstream of each Pier.

For the case of weaker discharge Q2, even 4 mm sediments are not suspended, resulting in an even weaker radial sorting. In addition, notice that most of the larger sediments, especially in GSD3, were not fully detached from the matrix and hence cannot be sorted. The situation observed in the field is closest to the image of the first row of Figure 14, which shows the results of GSD2 under Q1. Note that most of the visited gravel bed rivers have the closest geometric standard deviation (σ_g) to GSD2. Both the experiment and field observation confirm that the sorting upstream of the pier is almost identical across various aspect ratios. This proves that pier length has minimal or limited effects on the conditions of sorting upstream of the pier.

Figure 15 shows the conditions downstream of the piers. Whether scoured or deposited, clusters of fines are noticed to be formed directly downstream of the pier in several instances. In summary, the phenomenon occurred in 10 out of 16 runs in GSD2 and 6 in a total of 16 cases in GSD3. There are two mechanisms explaining the formation of these clusters. First, pier lengths were observed to have effects on the reduction in reconnection velocity and subsequently the decrease in turbulence downstream of the pier. Calmer flow downstream allows deposition of smaller sizes of fractions. This mechanism was well observed for GSD2 Pier2 to Pier4 on lower flows (Q2) and Pier3 and Pier4 for higher flows (Q1). For GSD3, the same mechanism was observed for high flows, as clusters were formed behind Pier3 and Pier4. However, this trend was reversed for low flows in GSD3, as clusters were formed only behind Pier1. Unlike the prior mechanism, clusters are formed downstream the shorter pier, since flow is too weak for the sediment from the upstream scour to reach the downstream side of the longer piers. Unlike some of the cases observed in the experiment, none of the visited piers have formed fine sediment clusters on their downstream sides. In the field, the downstream of all of the visited piers was characterized by loose rounded large sediments. This is because all of the visited piers

were subjected to a relatively larger discharge and faster approach velocity, such that the reconnection velocity is capable of selectively entraining fines and forming an armor on the downstream side of the pier. In terms of size distribution, the conditions of GSD2 Q1 P1, GSD2 Q1 P2, and GSD2 Q2 P1 are closest to what is observed onsite. As confirmed in the profile in Figure 12a, the location of the loose mound deposit is farther for the circular pier Pier1, compared to the longer pier Pier2, which is consistent with what was observed onsite.

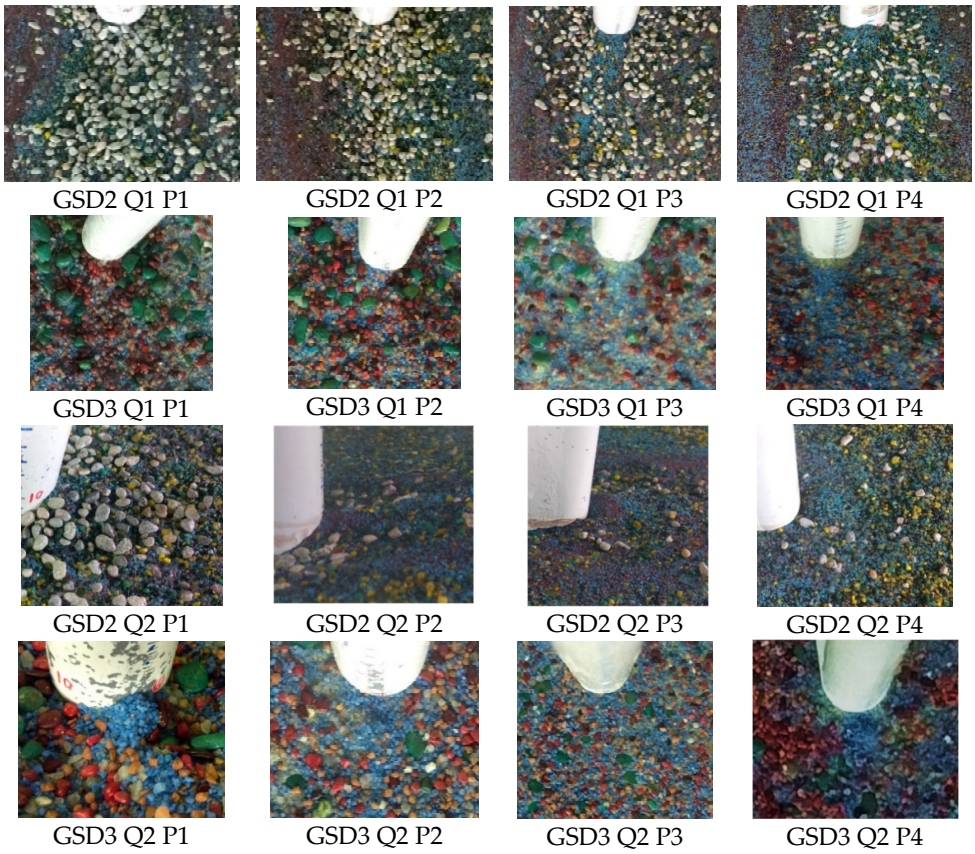

Figure 15. Situation just downstream of each Pier.

4. Discussions

The combined effects of aspect ratio and bed material grading were not clearly observed in the field, due to the variety in sediment size as well as flooding conditions among the visited rivers. Nonetheless, the observed effect of aspect ratio on field was replicated in the performed experiments. Based on the results of the flume experiments, the interaction between the process of sediment sorting and scouring is analyzed in this section. Longer piers have longer transition zones, affecting the condition just downstream the pier. Unlike the prominent effect on the downstream side, the conditions upstream of the pier are almost identical among different aspect ratios. It was observed that in GSD2, larger fractions are more mobile and are more likely to be transported around circular piers compared to other aspect ratios. In addition, due to the innate stability of GSD3, scour was not fully developed apart from circular piers. In the view of bridge pier safety, smaller and bigger aspect ratios each have pros and cons. Based on the experiments, we can say that scours are form most easily around circular piers, relative to longer piers. On the other hand, longer piers are more sensitive to flow orientation and are more prone to asymmetric scouring.

As previously discussed, the scour depth decreases dramatically with σ_g under clear-water scouring. This observation may be associated with the sorting of sediment along the scour slope upstream of the pier. Among the three bed materials used, a distinct feature was observed in GSD1, which represents uniform beds. The scours were formed by two slopes: one steep, almost vertical inner slope and another relatively milder outer slope, which is approximately equal to the internal angle of friction or static angle of repose (ϕ) of bed. This form was previously reported in numerous studies utilizing fine uniform bed materials. Regardless of nose shape, the outer slope angle was reported to be approximately equal to the bed material's ϕ, as reported by Lee, who investigated using a rectangular pier [34]. For uniform beds, as scour depth upstream of the pier increases, the extent also widens to maintain the static repose angle of the outer slope of the scour. The prior observations were not observed in sediment mixes. The feature of inner slope was notably missing from both sediment mixes utilized in this experiment, GSD2 and GSD3. Instead, the innermost area of the scour was observed to be lined with loose or clustered sediments from the larger-size fractions of the sediment mixture. This observation may explain the role of the larger fractions in deterring the propagation of scour both in terms of depth and area. We know that the area surrounding the pier nose is subjected to the combined effects of the downward force and the primary horseshoe vortex, making it the origin of scouring. Large sediments lining this area act as both velocity dissipators and armor coats inhibiting further excavation/erosion. Additionally, the angles of the scours formed on mixed sediments were found to be milder, decreasing with higher σ_g: GSD1 = 35.0°, GSD2 = 29.8°, and GSD3 = 21.0°. These values are the opposite of the expected trend, should we extend the observation in uniform sediments that scour angle is approximately equivalent to internal angle of friction of the bed material. Bagnold equated the bedload transport rate of a river to the product of per unit width stream power and transport efficiency, divided by the tangent of the static angle of friction of the bed material [35]. For identical rivers and flooding conditions, bed load rate is inversely proportional with the internal angle of friction. To confirm, the natural angles of repose of the sediment mixes were measured through the constant funnel method. The values of the static angles of friction are as follows: GSD1 = 33°, GSD2 =34°, and GSD3 = 34.8°. They were observed to be increasing with wideness of the size distribution, which was consistent with the observed amount of bed material transported.

We may attribute the difference between the natural angle of repose and the scour slope to several causes. For uniform sediments, the 2° difference is reasonably small and may be associated with the effect of water content. Although sands are idealized as cohesionless, this is not always the case in actual samples. For GSD2, the difference may be associated with the sorting of sediments along the slope. As scour develops, the sorting of sediments along the slope improves. With the deposition of larger sediment fractions on the bottom of the scour and additional finer materials supplied from the upstream, the mean diameter of the sediments along the slope is reduced. This results in a weaker internal angle of friction; hence, the scour angle follows. Unlike GSD2, GSD3 has sediment size fractions that are completely immobile despite the flow disturbance around the pier; therefore, sorting is rather partial. The mildness of the scour formed in GSD3 may be explained by the inherent stability of the mixture as bed material. The intensity of the downward force is insufficient to further excavate the bed and propagate the scour; hence, the development of the horseshoe vortex is also halted. The maximum depth created was also rather shallow to allow the bed to collapse and produce its natural angle of repose, a process which was observed for both GSD1 and GSD2.

Armoring is among the previously pointed-out products of sorting that influence scouring behaviors. As early as 1976, Ettema already cited armoring as a reason for scour depth reduction in mixed sediments subjected to clear-water scouring [11]. Ettema noted that the absence or collapse of armors formed within the scour holes would lead to deeper scours relative to unstratified uniform bed [36]. This result was echoed by Dey, as he coined the term secondary armor to refer to armors formed within scour holes [37]. A

more recent study by Pandey tackled the role of grain size distribution wideness (σ_g) in the dynamics of armoring and scour depth [25]. The study observed that the median size of armor (d50a) increases with σ_g. In turn, higher d50a results in more stable and shallower scour holes, which is consistent with Dey's previous observation. Melville and Sutherland related d50a as a function of larger-size fractions above d90 up to d99 [32]. Interestingly enough, the role of larger fractions is not only limited to armor formation but also extends to the general stability of beds. Mackenzie found that a slight difference in sediment size above d95 would have a significant impact on riverbed stability [38]. Like armoring in the main channel, the stability of secondary armor depends on movement of coarser particles. As described by Kothyari, armor formation is a nonstop process of successive development and collapse of sediment clusters [39]. Kothyari investigated scouring and armoring around abutments and noted that stable armor layers are rather uniform and have significantly smaller σ_g in comparison to the parent bed material. Kothyari's observations were observed actively in experiments on mixed beds during the development of the scour alongside the secondary armor inside of it.

All of the reviewed articles concerning scouring around bridge piers on non-uniform beds were performed on circular piers. However, knowing that armoring is a process highly dependent on cluster formation, the randomness of the sediment becomes extremely important. Prior scouring studies on uniform beds have determined that aspect ratio does not have a considerable effect on scouring depth, and this observation may be extended to scour asymmetry based on current results of performed experiments. However, it was observed that pier length to both scour depth and asymmetry becomes significant in the case of non-uniform beds. We know that scouring upstream of the pier grows radially, while it propagates along the piers' sides from upstream to downstream. Clusters and the subsequent armor formation become key elements in hindering the propagation in both depth and length, which in turn results in the asymmetry of scour holes. Longer piers have a greater tendency to have asymmetric scours, as piers act as dividers that completely separate the two sides of the channel. The contents of the bed are completely random; one side may have larger fractions and hence have more chances of forming clusters. In contrast, another side may have more fines and therefore have more parts that are easily entrained, leaving a larger scour. The effects of bed material randomness are magnified when clusters are formed and stabilized on either side. As a scour on one side continuously progresses, the other slows down or completely halts due to armoring. The difference in bed topology affects flow pattern. The side with deeper and longer scours has lesser flow resistance, and hence, it receives more discharge relative to the other side. This inequality does not only affect conditions of the bed along the side of the pier but also affects the condition downstream due to the conditions of reconnection.

Exposed coarse sediments were observed downstream of shorter piers. This observation is mainly due to the selective entrainment of finer fractions. This coarsening phenomenon can also be attributed to armoring. Apart from stability due to weight, the roughness of the uppermost layer helps dissipate velocity; therefore, the layer acts as an armor, shielding smaller sediments below and avoiding further degradation. Unlike the armors formed by sediment cluster formation, the stability of this armor is solely dependent on individual sediment weight. Although both are associated with armoring, the forming process of the two armors, upstream and downstream of the pier, is fairly different. As mentioned earlier, the stability of the armor formed due to the downward force and horseshoe vortex is highly dependent on cluster formation. These armors are initially mobile armors as scouring progresses, but they turn into static armors as sediment supply halts and scour finally stabilizes. On the other hand, the one formed downstream is completely formed due to selective entrainment. Due to the difference in the forming process and reasons for stability, it is anticipated that these two will also have a different response when the flow field suddenly changes. Since armoring upstream and on the sides of the pier is stable due to cluster formation, it requires higher velocity to initiate motion relative to individual sediments, as they act as a group. However, its stability is rather fragile.

Once the armor layer is broken, it is anticipated that scour will propagate drastically. On the other hand, the armor on the downstream end of the pier is individually stable. Therefore, once the net flow velocity in a certain direction surpasses the critical velocity of individual sediment, transportation initiates.

5. Conclusions

A total of nine (9) round-nose bridge piers of varying aspect ratios, along six (6) different gravel bed rivers in Japan, were visited. In these rivers, a common pattern related to scouring and sorting was observed. The features of the observed scour hole may be separated into three zones. Zone 1, the scour zone, which is located on the upstream end of the pier, is characterized by a steep downward sandy slope with gravel deposits on the lowest part. Zone 2, the transition zone, is the section along both pier sides, which is characterized by a relatively gentler positive slope and gradual increase in sediment size from upstream to downstream sides of the pier. More often than not, the elevations of the left and right sides of zone 2 are unequal. Zone 3, the mound zone, is the area downstream the pier characterized by a pile of rounded sediments, with noticeable absence of fines. Even though scouring and sorting are observed to be co-existing in a scour hole, the interaction of these two phenomena had yet to be clarified in previous literature.

The sorting and scouring patterns observed on sites were explained through the results of flume experiments. It was confirmed that maximum scour depth dramatically decreases with the wideness of the sediment distribution curve, indexed through geometric standard deviation (σ_g). Apparent asymmetry of the scour was also observed on both mixed-sediment beds, despite piers perfectly aligned with the flow. This observation proves that other factors such as grading affect scour shape. The number of cases where the location of the lowest point of the scour was shifted to further downstream was found to increase with σ_g. The number of cases where the location of the lowest point is outside the upstream cylindrical hemisphere was zero at uniform sediments GSD1 ($\sigma_g = 1.4$), three at GSD2 ($\sigma_g = 2.5$), and five at GSD3 ($\sigma_g = 5.2$). This will have implications for the extent and location of scour protection measures for local scouring around piers.

The three different bed materials used in this study have shown three unique scour-forming processes influenced by different mobility. The results of the experiments performed and literature review result in identifying two different kinds of armoring upstream and downstream the piers. Although both related to armoring, the two have distinct forming mechanisms and different factors for stability. The first type of armoring formed upstream is heavily dependent on clasts formation. The radial sorting of sediments on the upstream side of the pier provided a rather stable armor coat, which interferes with the propagation of the scour further downward, explaining the reduction in maximum scour depth relative to uniform bed. The upstream-to-downstream propagation of scour along the sides of the pier may explain the gradual decrease in fines on the surface, as well as the observed asymmetry of the scour. The type of armor found on the downstream end of the pier was formed through selective entrainment, which may clarify the absence of fines in this area. This armor is solely stable due to its weight, explaining why sediments on this region are relatively rather larger.

Through this, we can confirm that combined effects of grading of the bed material and piers' aspect ratio play an important role in the scour-forming process and alter the properties previously established in past literature.

In this study, there were brief periods of unsteady flows in between extended steady flows; nonetheless, the steady flow conditions were significantly longer than the unsteady intervals. However, an unsteady pattern of the discharge is considered to affect the sorting process. The relationship among the pattern of discharge, scouring, and sorting should be investigated. Moreover, the discharge in the flume was limited in this study; the runs were all within a clear-water scouring regime. Experiments to cover other cases need to be conducted in future.

Supplementary Materials: The following supporting information can be downloaded at: https://www.mdpi.com/article/10.3390/w14132066/s1, Figure S1: Four blunt-nosed cylindrical piers: (a) Graduated Piers of Varying Aspect Ratio; (b) Side Gradation; Figure S2: Setup of the flume for Experiment: (a) Planar Design; (b) Actual Condition; Figure S3: Cross-Section profile along line 1 for all aspect ratios and GSD (Q2, T4); Figure S4: Bed Topology Around Piers on GSD1 (Q2, T4); Figure S5: Bed Topology Around Piers on GSD2 (Q2, T4); Figure S6: Bed Topology Around Piers on GSD3 (Q2, T4).

Author Contributions: Conceptualization, T.C. and R.Q.; methodology, R.Q.; formal analysis, R.Q.; investigation, T.C. and R.Q.; resources, T.C.; writing—original draft preparation, R.Q.; writing—review and editing, T.C. and K.W.; supervision, T.C. and K.W. All authors have read and agreed to the published version of the manuscript.

Funding: This research received no external funding.

Institutional Review Board Statement: Not applicable.

Informed Consent Statement: Not applicable.

Conflicts of Interest: The authors declare no conflict of interest.

References

1. Wessel, P.; Smith, W.H.F. A Global, Self-Consistent, Hierarchical, High-Resolution Shoreline Database. *J. Geophys. Res. Solid Earth* **1996**, *101*, 8741–8743. https://doi.org/10.1029/96jb00104.
2. Milliman, J.D.; Meade, R.H. World-Wide Delivery of River Sediment to the Oceans. *J. Geol.* **1988**, *91*, 1–21.
3. Mohamed, Z.; Zeinab, Y.; Harun, C.; Firoz, A. A Review on The Methods Used to Reduce the Scouring Effect of Bridge Pier. *Energy Procedia* **2019**, *160*, 45–50. https://doi.org/10.1016/j.egypro.2019.02.117.
4. Enomoto, T.; Horikoshi, K.; Ishikawa, K.; Mori, H.; Takahashi, A.; Unno, T.; Watanabe, K. Levee Damage and Bridge Scour By 2019 Typhoon Hagibis In Kanto Region, Japan *Soils Found.* **2021**, *61*, 566–585. https://doi.org/10.1016/j.sandf.2021.01.007.
5. Chabert, J.; Engeldinger, P. *Etude des Affouillements Autour des Piles des Ponts;* Laboratoire National dâHydraulique: Chatou, France, 1956.
6. Melville, B.W.; Coleman, S.E. *Bridge Scour*; Water Resources Publication: Littleton, CO, USA, 2000.
7. Dey, S. *Fluvial Hydrodynamics*; Springer: Berlin, Germany, 2014. https://doi.org/10.1007/978-3-642-19062-9.
8. Francesco, C.; Roberto, G.; Costantino, M. Near-Bed Eddy Scales and Clear-Water Local Scouring Around Vertical Cylinders, *J. Hydraul. Res.* **2020**, *58*, 968–981. https://doi.org/10.1080/00221686.2019.1698668.
9. Sulaiman, M.; Tsutsumi, D.; Fujita, M.; Hayashi, K. Classification of Grain Size Distribution Curves of Bed Material and The Porosity. *Annu. Disaster Prev. Res. Inst.* **2007**, *50*, 615–622.
10. Nicollet, G.; Ramette, M. Affouillements Au Voisinage De Piles De Pont Cylindriques Circulaires. In Proceedings of the 14th IAHR Congress, Paris, France, 29 August–3 September, 1971; Volume 3, pp. 315–322.
11. Ettema, R. Influence of Bed Material Gradation on Local Scour. Master's thesis, University of Auckland, Auckland, New Zealand, 1976.
12. Baker, R.E. Local Scour at Bridge Piers in Non-Uniform Sediment. Master's thesis, the University of Auckland, Auckland, New Zealand, 1986.
13. Umeda, S.; Yamazaki, T.; Yuhi, M. An Experimental Study of Scour Process and Sediment Transport around a Bridge Pier with Foundation. In Proceedings of the 5th International Conference on Scour and Erosion (ICSE-5), San Francisco, CA, USA, 7–10 November 2010; pp. 66–75. https://doi.org/10.1061/41147(392)5.
14. Eghbali, P.; Dehghani, A.; Arvanaghi, H.; Menazadeh, M. The Effect of Geometric Parameters and Foundation Depth on Scour Pattern Around Bridge Pier. *J. Civ. Eng. Urban.* **2013**, *3*, 156–163.
15. Murtaza, G.; Hashmi, H.N.; Naeem, U.A.; Khan, D.; Ahmad, N. Effect of Bridge Pier Shape on Scour Depth at Uniform Single Bridge Pier. *Mehran Univ. Res. J. Eng. Technol*. **2018**, *37*, 539–544. https://doi.org/10.22581/muet1982.1803.08.
16. Vijayasree, B.A.; Eldho, T.I.; Mazumder, B.S.; Ahmad, N. Influence of Bridge Pier Shape on Flow Field and Scour Geometry. *Int. J. River Basin Manag*. **2019**, *17*, 109–129. https://doi.org/10.1080/15715124.2017.1394315.
17. Carling, P.A.; Kelsey, A.; Glaister, M.S.; Effect of Bed Roughness, Particle Shape and Orientation on Initial Motion Criteria. In *Sediment Transport in Gravel-Bed Rivers*; Thorne, C.R., Bathurst, J.C., Hey, R.D., Eds.; Wiley: Chichester, UK, 1992; pp. 23–37.
18. Fukuoka, S.; Osada, K. Sediment Transport Mechanism and Grain Size Distributions in Stony Bed Rivers. In Proceedings of the 33rd IAHR Congress: Water Engineering for A Sustainable Environment, Vancouver, BC, Canada, 2009; 505–512.
19. Mizutani, H.; Nakagawa, H.; Kawaike, K.; Zhang, H.; Lejeune, Q. Local scour and sediment sorting around an impermeable spur-dike with different orientations, In Proceedings of the 12th International Symposium on River Sedimentation (Isrs), Kyoto, Japan, 2–5 September 2013; pp. 879–890.
20. Zhang, H.; Nakagawa, H.; Local Scour and Sediment Sorting Around a Series of Groynes. *J. Jsnds* **2016**, *35*, 117–129.
21. Powell, D.M.; Progress in Physical Geography Patterns and Processes Of Sediment Sorting in Gravel-Bed Rivers. *Prog. Phys. Geogr*. **1998**, *22*, 1–32. https://doi.org/10.1177/030913339802200101.

22. Lanzoni, S.; Tubino, M.; Grain Sorting and Bar Instability. *J. Fluid Mech.* **1999**, *393*, 149–174. https://doi.org/10.1017/S0022112099005583.
23. Milhous, R.T. Sediment Transport in a Gravel-Bottomed Stream. Ph.D. Thesis, Oregon State University, Corvallis, OR, USA, 1973.
24. Pitlick, J.; Mueller, E.R.; Segura, C.; Cress, R.; Torizzo, M. Relation Between Flow, Surface-Layer Armoring and Sediment Transport in Gravel-Bed Rivers. *Earth Surf. Process. Landf.* **2008**, *33*, 1192–1209. https://doi.org/10.1002/esp.
25. Pandey, M.; Chen, S.C.; Sharma, P.K.; Ojha, C.S.P.; Kumar, V. Local Scour of Armor Layer Processes Around the Circular Pier in Non-Uniform Gravel Bed. *Water* **2019**, *11*, 1–10. https://doi.org/10.3390/w11071421.
26. Hjorth, P. Studies on The Nature of Local Scour in *Bull series A, No. 46*; Dept. of Water Resources Eng., Lund inst. Of Tech., University of Lund: Lund, Sweden, 1975.
27. Laursen, E.M.; Toch, A. *Scour around Bridge Piers and Abutments;* Bulletin No.4 Iowa Highway Research Board: Iowa City, IA, USA, 1956.
28. Melville, B.W.; Chiew, Y.-M. Time Scale for Local Scour at Bridge Piers. *J. Hydraul. Eng.* **1999**, *125*, 369–375. https://doi.org/10.1061/(ASCE)0733-9429(1999)125).
29. Wolman, M.G.; A Method of Sampling Coarse River-Bed Material *Am. Geophys. Union. Trans*. **1954**, *35*, 951–956.
30. Chiew, Y.M.; Melville, B.W. Local Scour Around Bridge Piers *J. Hydraul. Res.* **1987**, *25*, 1, 15–26.
31. Barnes, H.H., Jr. Roughness Characteristics of Natural Elements. *U.S. Geol. Surv. Water-Supply Pap*. **1967**, 1849. https://doi.org/10.3133/wsp1849
32. Melville, B.W.; Sutherland, A.J. Design Method for Local Scour at bridge Piers. *J. Hydraul. Eng*. **1988**, *114*, 1210–1226. https://doi.org/10.1061/(ASCE)0733-9429(1988)114:10(1210)
33. Staudt, F.; Mullarney, J.C.; Pilditch, C.A.; Huhn, K. Effects of Grain-Size Distribution and Shape on Sediment Bed Stability, Near-Bed Flow and Bed Microstructure. *Earth Surf. Process. Landf.* **2019**, *44*, 1100–1116. https://doi.org/10.1002/esp.4559.
34. Lee, S.O.; Sturm, T.W. Effect of Sediment Size Scaling on Physical Modeling of Bridge Pier Scour. *J. Hydraul. Eng*. **2009**, *135*, 793–802. https://doi.org/10.1061/(ASCE)HY.1943-7900.0000091.
35. Bagnold, R.A. An Approach to the Sediment Transport Problem from General Physics. Geological Survey Professional Paper, U.S. Government Printing Office, Washington, D.C., USA, 1967. https://doi.org/10.3133/pp422I
36. Ettema, R. *Scour at bridge piers. Rep*. *No. 216*; School of Engineering, University of Auckland: Auckland, New Zealand, 1980.
37. Dey, S.; Raikar, R.V. Clear-Water Scour at Piers in Sand Beds with an Armor Layer of Gravels. *J. Hydraul. Eng.* **2007**, *133*, 703–711. https://doi.org/10.1061/(ASCE)0733-9429(2007)133:6(703).
38. MacKenzie, L.G.; Eaton, B.C. Large Grains Matter: Contrasting Bed Stability and Morphodynamics During Two Nearly Identical Experiments. *Earth Surf. Process. Landf.* **2017**, *42*, 1287–1295. https://doi.org/10.1002/esp.4122.
39. Kothyari, U.C.; Hager, W.H.; Oliveto, G. Generalized Approach for Clear-Water Scour at Bridge Foundation Elements. *J. Hydraul. Eng.* **2007**, *133*, 1229–1240. https://doi.org/10.1061/(ASCE)0733-9429(2007)133:11(1229).